





# Evolution of Pore Reorganization of Porous Silicon

Sarah Sanz<sup>1</sup> , Yves Patrick Botchak Mouafi<sup>1</sup> , Giso Hahn<sup>1</sup> ,  
Gabriel Micard<sup>1</sup> , and Barbara Terheiden<sup>1</sup>

University of Konstanz, Germany

\*Correspondence: Sarah Sanz, [sarah.sanz-alonso@uni-konstanz.de](mailto:sarah.sanz-alonso@uni-konstanz.de)

**Abstract.** To obtain a closed and smooth surface of a porous Si layer for an epitaxial growth of a silicon wafer, the porous Si must be reorganized. To understand the reorganization process, the evolution of the pores is investigated in this contribution. The reorganization process is interrupted at different stages and cross-sectional SEM images are taken to evaluate the change in pore size and shape during reorganization. Additionally, the stress is measured using XRD. At the beginning of the reorganization of the pores, the as-etched columnar pores with diameters of about 5 nm become coarser with larger diameters. At temperatures above 900°C, the surface closes and thus becomes smooth. In addition, the form of the pores starts to change from columnar to round with diameters between 55-65 nm. When the highest temperature of 1100°C is reached, the columnar pores have disappeared and the pores are round and faceted. With an additional plateau time of up to 20 min, there is no visible change in pore faceting. The as-etched sample shows tensile stress and the sample annealed at 700°C is nearly unstressed. When the temperature is increased beyond 900°C, the stress is compressive and no further change is visible.

**Keywords:** Porous Silicon, Reorganization, Stress Measurement

## 1. Introduction and Experimental

In 1956, Uhler [1] first discovered the electrochemical etching of porous silicon while attempting electrochemical polishing. Later, Brendel [2] used porous silicon to produce epitaxially grown silicon films on top. This requires reorganizing the porous silicon at high temperatures to obtain a closed and smooth surface. In this contribution, the evolution of the reorganization is investigated in order to understand the reorganization process and possibly optimize it.

The porous silicon layers were prepared by anodic electrochemical etching of 156.5×156.5 mm<sup>2</sup> full square, (100)-oriented highly boron-doped (p-type) Czochralski-grown Si (Cz-Si) with a resistivity of 11-12 mΩcm in a HF:H<sub>2</sub>O:2-propanol solution of 1:1:1. After etching, the reflectance in the visible and up to the infrared spectral range was determined at 30×30 points across each sample to obtain the thickness and porosity of the porous silicon layer [3]. Reorganization was performed in an H<sub>2</sub> and Ar atmosphere at a pressure of 8.8 Torr, a peak temperature of up to 1100°C and a plateau time of up to 20 min. The reorganization process was interrupted at various stages to analyze the evolution of pore size and shape. Fig. 1 shows the temperature profiles of the reorganization process interrupted at different stages. The reorganization interruptions at temperatures >700°C are followed by an unavoidable cooling step of about 30 min.

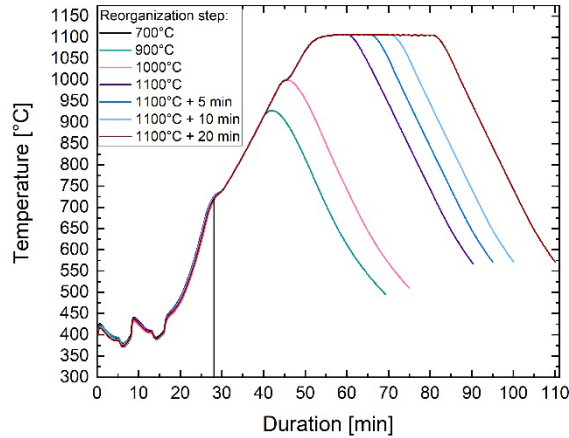
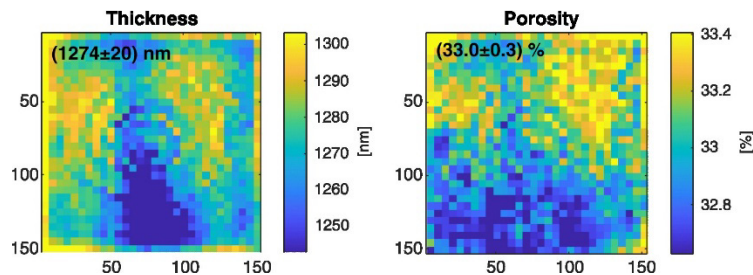


**Figure 1.** Temperature profiles of the reorganization processes interrupted at different reorganization stages, for temperatures >700°C followed by an unavoidable cooling step of about 30 min.

After reorganization, cross-sectional scanning electron microscopy (SEM) images were taken to evaluate the change in pore size and shape during reorganization. Wafer strain was determined by X-ray diffraction (XRD) using a Bruker D8 Advance X-ray diffractometer equipped with a copper (Cu) target X-ray tube operating at 40 kV and 40 mA. The diffraction patterns were recorded in the  $2\theta$ - $\theta$  mode in the  $2\theta$  range from  $69^\circ$  to  $69.5^\circ$ , with a step size of  $0.001^\circ$  to investigate the shift of the (400) peak caused by the porous silicon on top of the non-etched wafer.

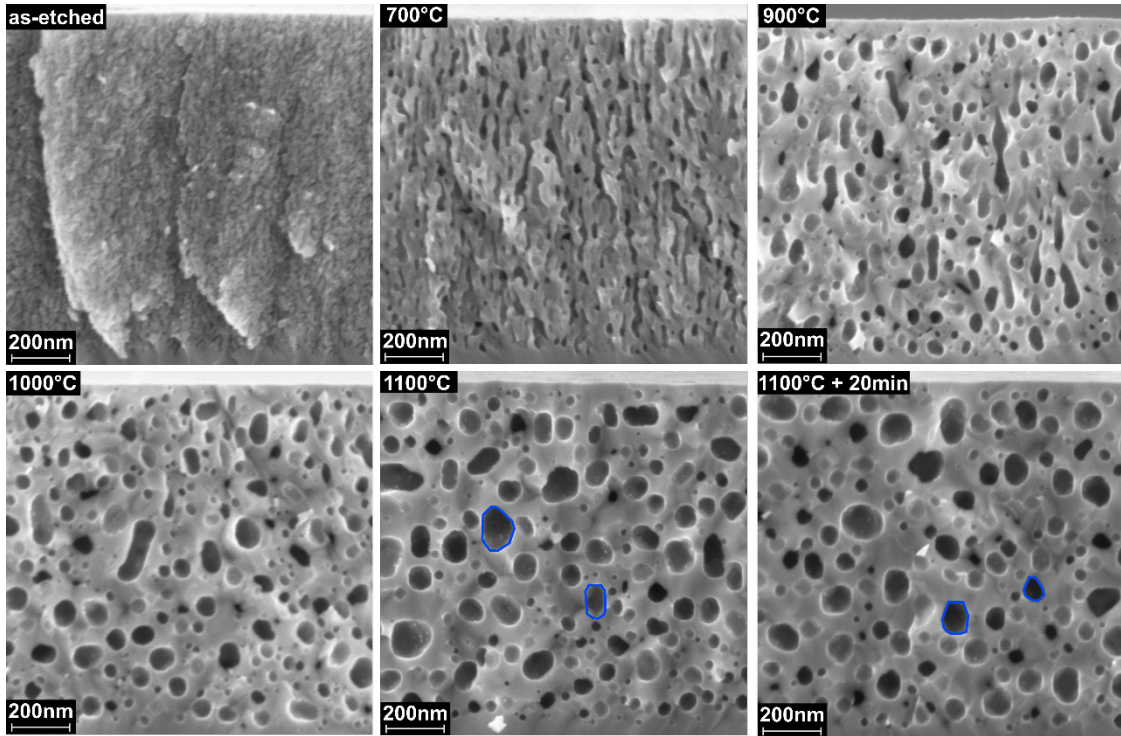
## 2. Results and Discussion

Fig. 2 shows the thickness and porosity maps of a typical porous Si layer obtained from reflectance spectra at  $30 \times 30$  points across the wafer area [3]. The mean values and the standard deviation across the wafer are shown in brackets. This standard deviation is a measure of the uniformity.



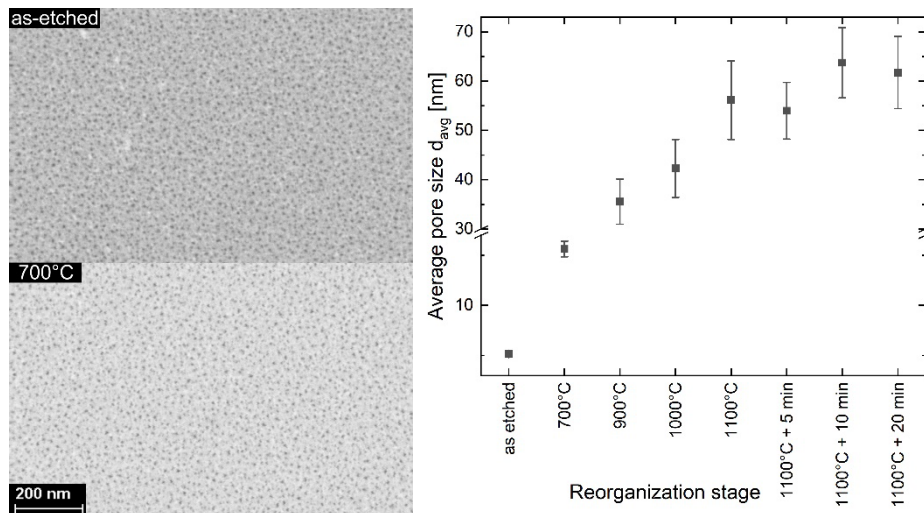
**Figure 2.** Spatially resolved maps of porosity and layer thickness of an as-etched porous Si layer. The standard deviations indicate the spatial variation across the wafer ( $30 \times 30$  points) being a measure of its uniformity.

Fig. 3 shows the cross-sectional SEM images after different reorganization stages. The first image shows the as-etched state, where the surface is not closed and the pores have a columnar shape. At a temperature of  $700^\circ\text{C}$ , individual pores can be identified, the columnar pores become coarser, and the holes in the surface become larger. At a temperature of  $900^\circ\text{C}$ , the surface is closed. In addition, the form of the pores starts to change from columnar to round. At a temperature of  $1000^\circ\text{C}$ , the surface is already closed and appears to be relatively smooth. The columnar shape of the pores has disappeared and the pores are rounded.



**Figure 1.** Cross-sectional SEM images of reorganized porous Si interrupted at different reorganization stages. Blue lines indicate examples of faceted pores.

At 1100°C, which corresponds to typical reorganization temperature, the pores are rounder than at 1000°C and faceted, as indicated by the blue lines in Fig. 3. With an additional plateau time of up to 20 min, there is no visible change in the SEM image. This suggests that the pores stay stable with these porous Si parameters and the investigated durations.



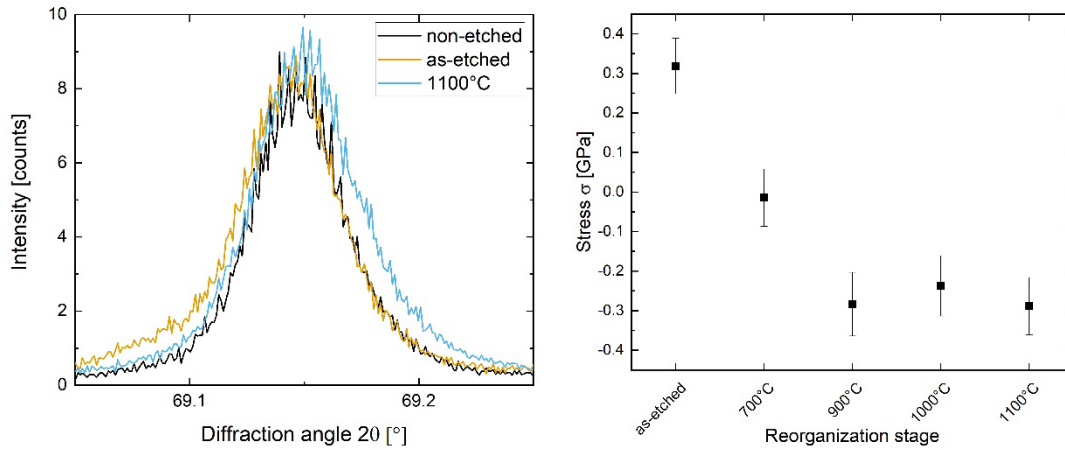
**Figure 2.** Left: Top view SEM images of the as-etched and the sample at 700°C. Right: Average pore size calculated from the pore size distribution over the reorganization stage at which it was interrupted.

Fig. 4 right shows the average pore size for the different reorganization stages. For the as-etched state and 700°C, the pore sizes are determined from the wafer top view SEM image where each black spot represents one pore, as shown in Fig. 4 left. The other average pore sizes are calculated using a lognormal fit to the pore size distribution. The exact calculation is discussed elsewhere [4]. Due to the preparation of the SEM samples, the pores are not necessarily cut in the center of the pores and thus the extracted area of the pores is underestimated. However, together with the error bars indicating the variance of the lognormal fit, the

determined pore sizes are a reliable measure of the real size.

It can be seen that the initial average pore size of about 5 nm increases slowly at 700°C, then increases to >30 nm at 900°C, and finally reaches a value between 55-65 nm at 1100°C almost independent of the holding time. This indicates that the reorganization is completed and stable after few minutes at 1100°C. The increase in average pore size correlates with the onset of pore faceting at 900°C and further faceting at higher temperatures.

Fig. 5 left shows the determined XRD data for a non-etched wafer, for the as-etched sample and the sample reorganized at 1100°C. A small angle shift is observed, with the peak shifting to smaller angles for the as-etched wafer, indicating tensile stress. The peak of the reorganized wafer is shifted to higher angles, indicating compressive stress.



**Figure 5.** Left: XRD data of a non-etched wafer, the as-etched sample and the sample at 1100°C. Right: Calculated stress over the reorganization stage at which it was interrupted.

Using the Bragg equation  $n \cdot \lambda = 2d \cdot \sin(\theta)$ , the interplane distances  $d$  and their changes due to mechanical stresses can be determined. The strain  $\epsilon$  is calculated directly from the XRD peak displacement  $\Delta\theta$  using the relationship  $\epsilon = \Delta\theta \cdot \pi / 180 \cdot \cot(2\theta)$  [5], where  $\Delta\theta$  is the difference in peak position between the strained and unstrained state and  $\theta$  is the angle of the unstrained state. The stress  $\sigma$  is then calculated using Young's modulus of silicon  $E = 169$  GPa [6]. Fig. 5 right shows the calculated stress over the reorganization stage. The as-etched sample is stressed, but at 700°C the sample is nearly unstressed. At higher temperatures the stress changes direction and increases again. However, no change in stress is visible when the temperature is increased beyond 900°C.

### 3. Conclusion

In conclusion, this study investigated the reorganization process of porous silicon layers using SEM images and XRD data. The findings provided insights into the evolution of pore size, surface morphology, and mechanical stress during the reorganization stages. The SEM images showed a progression from an open, columnar pore structure to closed, round pores, with distinct changes in morphology occurring at different temperatures. The transition to round pores and pore faceting becomes prominent at temperatures above 900°C, indicating the completion of the reorganization process. Additionally, the stability of the pores was demonstrated by the absence of visible changes in SEM images with extended holding times at 1100°C. The analysis of the average pore size showed an increase from about 5 nm at the initial stage to a stabilized range of 55-65 nm at 1100°C. This suggests a correlation between pore enlargement and pore faceting. XRD data gave insight into the mechanical stresses experienced by the porous Si layers, with the transition from tensile to compressive stress observed during the reorganization process. Overall, these findings contribute to a deeper understanding of the

reorganization dynamics of porous Si layers. Further research could explore additional parameters that influence the reorganization process.

## Data availability statement

The data that support the findings of this study and details on the measurement setup are available from the corresponding author upon reasonable request.

## Author contributions

**Sarah Sanz:** Investigation, Conceptualization, Formal analysis, Writing - Original Draft; **Yves Patrick Botchak Mouafi:** Investigation, Formal analysis, Conceptualization, Writing - Original Draft; **Giso Hahn:** Review, Editing, Supervision; **Gabriel Micard:** Software, Writing - Original Draft; **Barbara Terheiden:** Conceptualization, Supervision, Funding acquisition, Project administration.

## Competing interests

The authors declare no competing interests.

## Funding

Part of this work was financially supported by the German Federal Ministry for Economic Affairs and Climate Action (FKZ 03EE1082B, 03EE1117B). The content is the responsibility of the authors.

## Acknowledgement

The authors would like to thank Barbara Rettenmaier for technical support.

## References

- [1] A. Uhlir, "Electrolytic shaping of germanium and silicon", *Bell System Technical Journal*, 35, 2, pp. 333–347, 1956, <https://doi.org/10.1002/j.1538-7305.1956.tb02385.x>
- [2] R. Brendel, "A novel process for ultrathin monocrystalline silicon solar cells on glass", *Proceedings of the 14<sup>th</sup> EUPVSEC*, Barcelona, Spain, 1997, pp. 1354-1358.
- [3] G. Micard, Y.P. Botchak Mouafi, B. Terheiden, "Non-destructive spatially resolved characterization of porous silicon layer stacks", *AIP Conference Proceedings* 2826, 120002, 2023, doi: <https://doi.org/10.1063/5.0141239>
- [4] G. Müller, M. Nerding, N. Ott, H.P. Strunk, R. Brendel, "Sintering of porous silicon", *Physica Status Solidi (a)*, 197, 1, pp. 83–87, 2003, doi: <https://doi.org/10.1002/pssa.200306472>
- [5] L. Spieß, "Moderne Röntgenbeugung", Vieweg+Teubner, 2009, p. 333.
- [6] M.A. Hopcroft, W.D. Nix, T.W. Kenny, "What is the Young's Modulus of Silicon?", *J. Microelectromec. Sys.*, 19, 2, pp. 229-238, 2010, doi: <https://doi.org/10.1109/JMEMS.2009.2039697>